Cement & Concrete Composites 30 (2008) 863–871

Contents lists available at ScienceDirect

Cement & Concrete Composites

journal homepage: www.elsevier.com/locate/cemconcomp

Evaluation of crack opening performance of a repair material with strain hardening behavior

Ahmed Kamal [a,b,*], Minoru Kunieda [a,1], Naoshi Ueda [a,2], Hikaru Nakamura [a,3]

[a] Department of Civil Engineering, Nagoya University, Chikusa-ku, Nagoya 464-8603, Japan
[b] Structural Civil Engineering Department, Cairo University, Egypt

ARTICLE INFO

Article history:
Received 22 December 2007
Received in revised form 18 August 2008
Accepted 18 August 2008
Available online 30 August 2008

Keywords:
UHP-SHCC
Uniaxial tensile test
Zero-span tensile test
Repaired RC beams

ABSTRACT

One of the novel mechanical properties of strain hardening cementitious composites (SHCC) is that they exhibit multiple fine cracks and strain hardening in tension. This promotes the use of SHCC as an effective repair material, because penetration of substances through the fine cracks is greatly reduced. Most research on SHCC has focused on its behavior and results obtained from uniaxial tensile tests. However, the crack distribution of the repair material (SHCC) layer is more concentrated adjacent to an existing crack in a substrate. So the design procedure considering the crack opening, which represents the potential for localized fracture, should be established for appropriate material selection. In this paper, the performance of SHCC as a repair material was assessed through three tests: uniaxial tensile tests; zero-span tensile tests; and flexural tests of RC beams repaired with SHCC. Comparisons between crack opening performances and the observed crack patterns of the three tests were conducted. The crack opening and crack pattern obtained from the zero-span tensile tests were similar to those of the repaired beam specimens. According to the zero-span tensile tests, the performance of cracking behavior of the repair material on an existing crack can be estimated. On the other hand, the deformation capacity of SHCC obtained from the uniaxial tensile tests cannot be directly applied to the design of surface repair application.

1. Introduction

Most civil engineers and construction industry experts have recognized the deterioration problem of aged RC structures in the world. The common forms of deterioration of those structures start from or near the surface [1]. The quality of the near-surface material determines the rate at which aggressive gases and solutions will penetrate. This rate of penetration is one of the main factors that determine the durability of the structure. The careful design of surface repairs can increase the service life of deteriorated structures.

One of the most important factors affecting on the successful repair of structures is the selection of repair material. Compatibility between substrate and repair material is one of the most important factors in selection of repair material. Cement-based materials are generally suitable for repairing concrete structures due to their compatible mechanical and physical properties (e.g. coefficient of thermal expansion, fracture energy, permeability), as well as other important considerations such as cost, availability, and constructability [2]. Recently, different types of cement-based composites have been developed to control mechanical properties, such as compressive strength, tensile strength, and the strain at tensile strength. In the past decade, fiber reinforced cementitious composites with higher ductility such as strain hardening cementitious composites (SHCC) have been developed. This progress has been due to the developments in fiber, matrix, and process technology, as well as better understanding of the fundamental micromechanics governing composite behavior [3]. SHCC promises to be used in a wide variety of civil engineering applications, as summarized in Japan Concrete Institute (JCI 2002) [4] and by Kunieda and Rokugo [5]. One of the most promising areas of application of this material is in the repair of concrete structures. Several investigations on the advantages of structures repaired by SHCC have been carried out. Lim and Li [6] found the mechanical advantages of an interface crack trapping mechanism within SHCC/RC composites. Horii et al. [7], Li [8], and Li et al. [9] applied SHCC to the repair or retrofit of concrete structures, and confirmed the effect of ductility of the repair materials on the structural performance. The effects of surface preparation on the fracture behavior of SHCC/RC composites

* Corresponding author. Address: Department of Civil Engineering, Nagoya University, Chikusa-ku, Nagoya 464-8603, Japan. Tel.: +81 52 789 4484; fax: +81 52 789 1664.
E-mail addresses: eng_ahmedka@yahoo.com (A. Kamal), kunieda@civil.nagoya-u.ac.jp (M. Kunieda), ueda@civil.nagoya-u.ac.jp (N. Ueda), hikaru@civil.nagoya-u.ac.jp (H. Nakamura).
[1] Tel./fax: +81 52 789 4633;
[2] Tel.: +81 52 789 1664; fax: +81 52 789 4635.
[3] Tel.: +81 52 789 1664; fax: +81 52 789 5690.

0958-9465/$ - see front matter © 2008 Elsevier Ltd. All rights reserved.
doi:10.1016/j.cemconcomp.2008.08.003

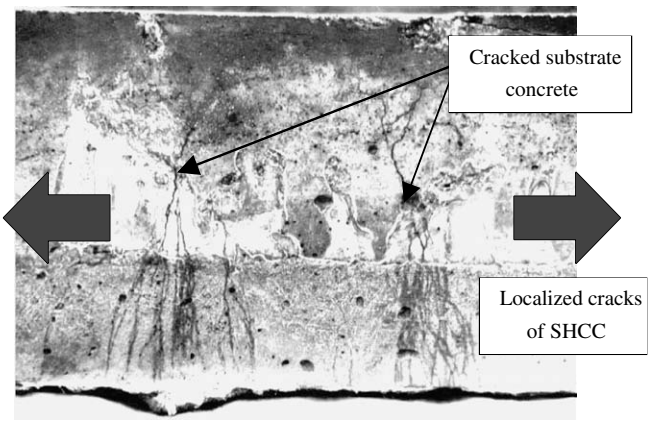

Fig. 1. Limited crack distribution of SHCC near to existing cracks of substrate concrete.

were discussed by Kamada and Li [10]. Li [11] also addressed the required properties for repair materials to obtain durable repaired concrete structures.

Most of these investigations concentrated on the global behavior of the repaired members. They have taken into account the advantages of high ductility of SHCC itself, which can be evaluated by uniaxial tensile tests or flexural tests. However, the boundary conditions of uniaxial tensile tests or flexural tests of SHCC materials are different from the existing ones in repair or retrofit applications. In repair applications where there is an existing crack within the substrate, it is well known that the crack distribution within the repair material (SHCC) is limited near to the existing crack, as shown in Fig. 1. So the design procedure considering the opening of the crack in the substrate (hereafter referred to as crack opening), which represents resistance against the localized fracture, should be established for appropriate material selection. Kunieda et al. [12] and Rokugo et al. [13] showed the localized fracture of SHCC in patch repair systems, experimentally and analytically. Kamal et al. [14] proposed the zero-span tensile test to evaluate the crack opening performance of the repair material on a substrate with an existing crack.

In this study, the attention is focused on using SHCC as a surface repair material which is usually used to increase the durability of the repaired structure. The performance of a surface repair material was assessed through the following three tests: uniaxial tensile tests; zero-span tensile tests; and flexural tests of RC beams repaired by SHCC. Comparisons are made between the crack opening performances and observed crack patterns of the three tests.

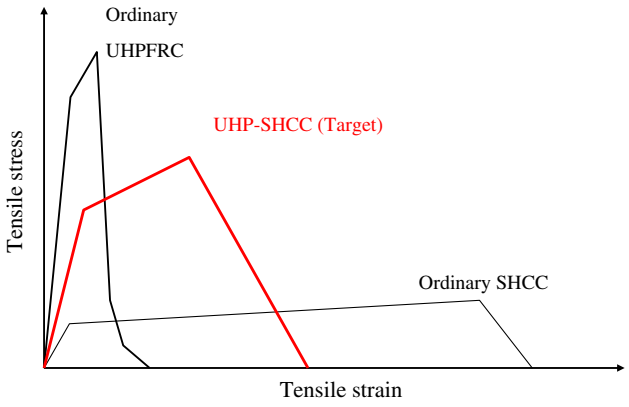

Fig. 2. A schematic image of UHP-SHCC material tensile behavior compared to that of other materials.

2. Repair materials

A new strain hardening composite, ultra high performance strain hardening cementitious composite (UHP-SHCC), with a dense matrix was developed and tested by Kunieda et al. [15]. This material combines excellent protective performance, similar to that of ultra high performance fiber reinforced concrete (UHPFRC), with a significantly higher tensile strain hardening (up to 2%) at peak strength. Fig. 2 shows the general behavior of UHP-SHCC in uniaxial tensile test compared to that of ordinary SHCC and ordinary UHPFRC.

UHP-SHCC was used as a repair material in this study. Three types of UHP-SHCC with different fiber content (0.5%, 1.0% and 1.5% in volume) were adopted. Table 1 shows the mix proportions of the three mixes. Water to binder (W/B) ratio was 0.18. Low-heat Portland cement was used, and 20% of the cement content was replaced by silica fume. Quartz sand with diameter less than 0.5 mm was used as a fine aggregate. High strength polyethylene (PE) fibers were chosen for this material. The diameter of fibers was 0.012 mm and the fiber length was 6 mm.

3. Uniaxial tensile test

3.1. Uniaxial tensile test setup

Uniaxial tensile tests with fixed boundary setup were conducted on five dumbbell-shaped specimens (tested cross-section: 10×30 mm) for each type of UHP-SHCC at 14 days after casting. In the tests, a Pi-type displacement transducer was glued on each of two surfaces of the specimen to measure the displacement opening of the specimen, as shown in Fig. 3. Gauge length of the transducers was 100 mm and the sensitivity of each transducer was about 1/2000 mm. The capacity of the transducers was equal to ±5 mm. The load was measured by load-cell having the capacity of 50 kN.

Table 1
Mix proportions of substrate concrete and UHP-SHCCs

Material	Water/binder[a]	Unit content (kg/m^3)								
		Water	Cement	Silica fume	Fine aggregate	Coarse aggregate	AE water reducing agent	Super-plasticizer	Air reducing agent	Fiber content (6 mm)
Substrate concrete	0.63	185.00	293.65	–	842.57	919.23	2.94	–	–	–
UHP-SHCC(0.5)[b]	0.18	266.53	1352.9	338.24	169.12	–	–	33.82	7.44	4.85
UHP-SHCC(1)	0.18	265.12	1345.8	336.45	168.22	–	–	33.64	7.40	9.70
UHP-SHCC(1.5)	0.18	263.71	1338.6	334.66	167.3	–	–	33.47	7.36	14.55

[a] Binder means cement + silica fume.
[b] Number in parentheses indicates volume fraction of fibers (%).

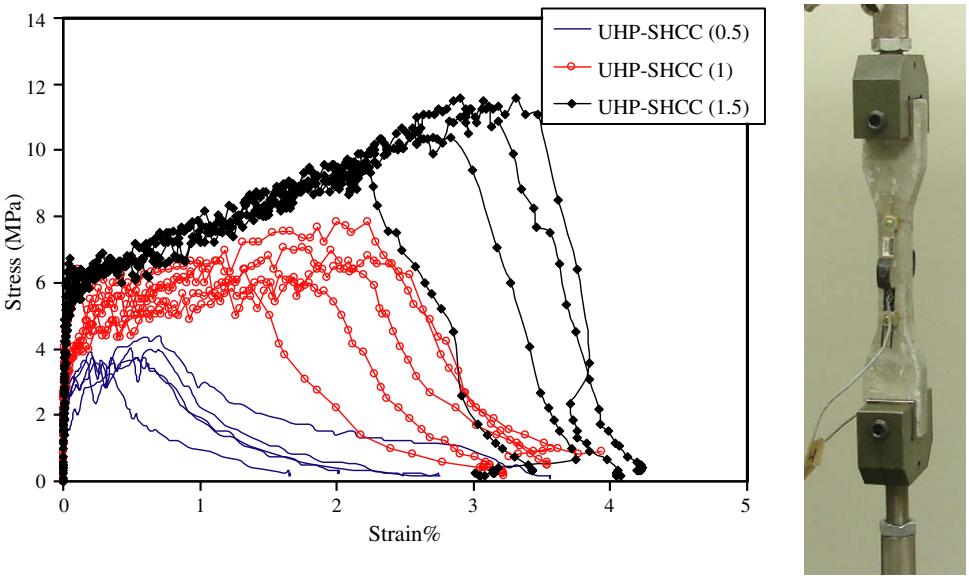

Fig. 3. Stress–strain relationship for uniaxial tensile tests of UHP-SHCC materials.

Table 2
Averaged mechanical properties of UHP-SHCCs at 14 days

Mechanical property	Material		
	UHP-SHCC(0.5)	UHP-SHCC(1)	UHP-SHCC(1.5)
Compression strength (MPa)	94	94	96
Young's modulus (GPa)	33.8	31	31.5
Tensile strength (MPa)	3.8	6.9	10
Strain at tensile strength (%)	0.58	1.76	2.8

3.2. Uniaxial tensile test results

Fig. 3 shows the stress–strain relationship measured from the uniaxial tensile tests. All UHP-SHCCs exhibited significant strain hardening. The averaged tensile strength and strain at the tensile strength of the UHP-SHCCs at 14 days are summarized in Table 2. As shown in this table, the tensile strength and the strain capacity depend on the fiber content of the material. The averaged strain capacity of UHP-SHCCs ranged from 0.58% to 2.8% and the tensile strength ranged from 3.8 to 11 MPa.

For the observed crack pattern, multiple fine cracks were observed along the length of specimens. The number of cracks also depended on the fiber content of the material, as shown in Fig. 4.

For compression properties of each mix design, five cylindrical specimens of $\varnothing$ 50 $\times$ 100 mm were also tested at 14 days after the casting. Table 2 shows the averaged compressive strength and Young's modulus. As shown in Table 2, no significant effect was observed of the fiber content on the averaged compressive strength of the different mixes of UHP-SHCCs. The averaged compressive strength ranged from 94 to 96 MPa and the Young's modulus ranged from 31 to 34 GPa.

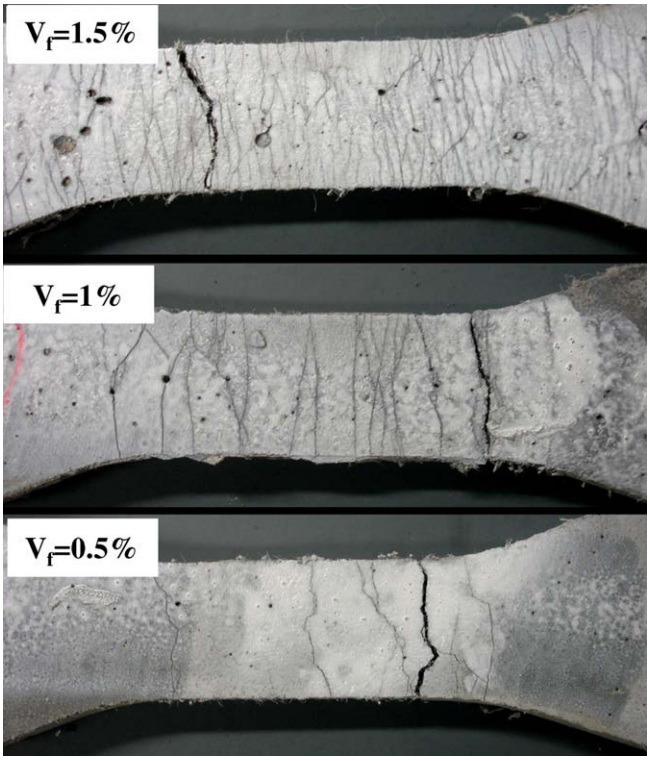

Fig. 4. Crack pattern of uniaxial tensile tests.

4. Zero-span tensile tests

4.1. Zero-span tensile test setup

Zero-span tensile test is a new proposed tensile test with special boundary conditions that reflect those of surface repair applications, as shown in Fig. 5. The main concept is to conduct the tensile test on a very short span to evaluate the resistance against localized fracture of the surface repair material. The basic idea of the zero-span tensile test proposed in this study is based on the test method for surface coating materials with a thin layer such as epoxy painting, which is specified in JSCE-K-532 [16].

In this study, zero-span tensile tests were used to evaluate the resistance of UHP-SHCC material in surface repair applications against the localized fracture. Fig. 6 shows the setup of the tests. The size of the UHP-SHCC specimens was 100 $\times$ 100 mm with a thickness of 10 mm, which is the same thickness as the repair layers applied to RC beams in the following section, and also the same thickness as that of the dumbbell-shaped specimens for the uniaxial tensile tests in previous section. Steel plates with thickness of

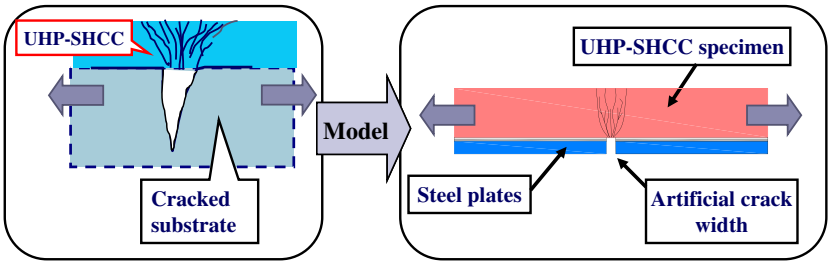

Fig. 5. Concept of the zero-span tensile test.

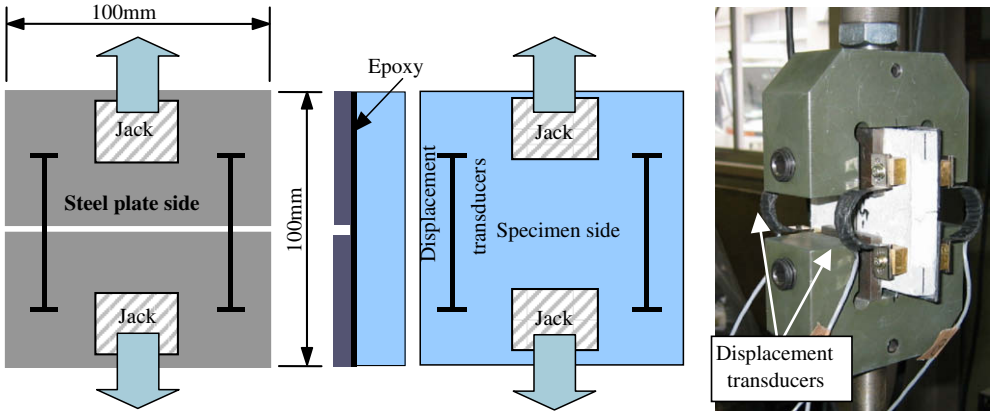

Fig. 6. Test setup for zero-span tensile tests.

3 mm were glued on the UHP-SHCC specimen by epoxy adhesive as shown in the test setup. The other substrates made of mortar or concrete that represent a similar substrate in existing concrete structures involve a surface preparation to obtain good bonding between repair material and the substrate. The procedures on surface preparation, however, would impart much work to the test method. In addition, insufficient bond properties induce delamination at the interface between repair material and the substrate, which gives the potentially misleading result of a more widely distributed cracked area, as shown in Fig. 7. In order to reduce the influence of the bond property on the crack opening performance of a repair material, perfectly bonded steel plates were used in this study. The artificial crack (i.e. the gap between the steel plates) should reflect the crack width of the cracked substrate. In this study, however, the most severe condition where an artificial crack width of 0 mm was used to induce localized fracture. It was clarified in previous study that the number of cracks adjacent the artificial crack and the measured opening displacement increase with increasing width of the artificial crack width [14]. Zero-span tensile test setup may cause some secondary moment because the vertical section of a specimen is not symmetrical in terms of stiffness due to the existence of steel plate attached to UHP-SHCC. In past research works [14], the effect of the secondary moment on the test results was investigated through various combinations between steel plate thicknesses (1, 3, and 5 mm) and repair material thickness (10, 15, and 20 mm). In these conditions, no significant effects of secondary moments were observed.

Four specimens of each type of UHP-SHCC with different volume fraction of fibers were tested by the zero-span tensile test. In these tests, two Pi-type displacement transducers were glued on each surface to measure the opening displacement at the artificial crack (i.e. two transducers were fixed on the specimen side and the two other transducers were fixed on the steel plate side), as shown in Fig 6. The measurement length of the transducers was 50 mm and the sensitivity of each transducer was about 1/2000 mm. The loading rate was about 0.2 mm/min, and the loading was terminated when the displacement was over 2 mm, which was equal to the capacity of the transducers. The load was measured by load-cell having the capacity of 50 kN. All tests were carried out during the age of 14 days.

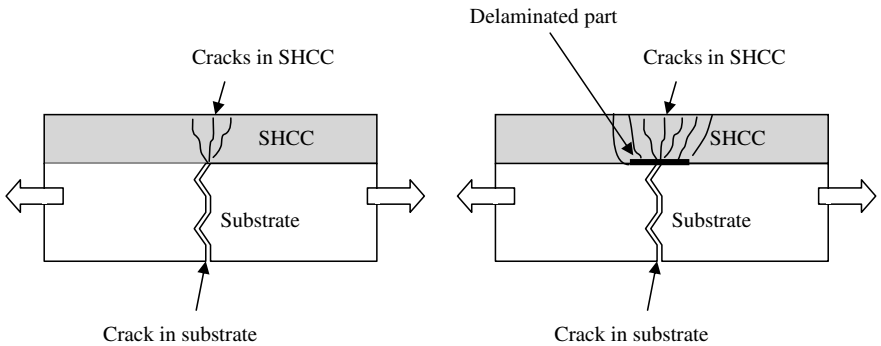

Fig. 7. Effect of delamination on the crack distribution in SHCC/RC composite.

4.2. Zero-span tensile test results

Fig. 8 shows the measured load–opening displacement curves through the zero-span tensile tests for UHP-SHCCs with different fiber volume contents. The measured opening displacement at the peak load, avoiding the first cracking load which is affected by strength properties of epoxy layer, is defined as the crack opening performance of the repair material. This point corresponds to the initiation of localized fracture as the carrying load capacity starts decreasing [14], as shown in Fig. 8. Note that crack opening performance means resistance against localized fracture of repair material. Regarding the scatter of the test results, the load values had a large scatter especially for UHP-SHCC with high fiber volume content, as indicated in Fig. 8. However, the scatter of crack opening defined as the displacement at maximum load was smaller compared to the scatter of load values. The results of all zero-span tensile tests are shown in Fig. 8.

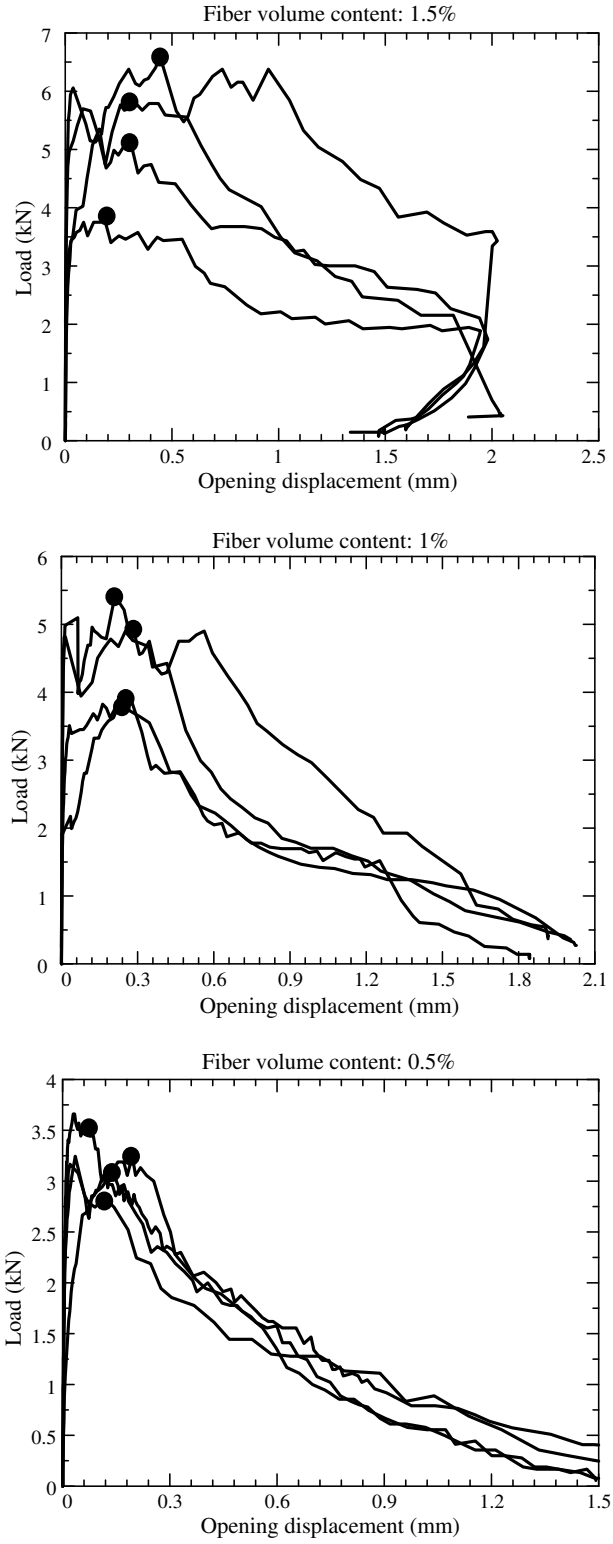

Fig. 8. Load–displacement curves obtained from zero-span tensile tests of UHP-SHCC.

Table 3
Averaged crack opening obtained from zero-span tensile tests of UHP-SHCCs

Material	UHP-SHCC(0.5), V_f = 0.5%	UHP-SHCC(1), V_f = 1%	UHP-SHCC(1.5), V_f = 1.5%
Crack opening (mm)	0.124	0.237	0.297
Standard deviation	±0.046	±0.0162	±0.095

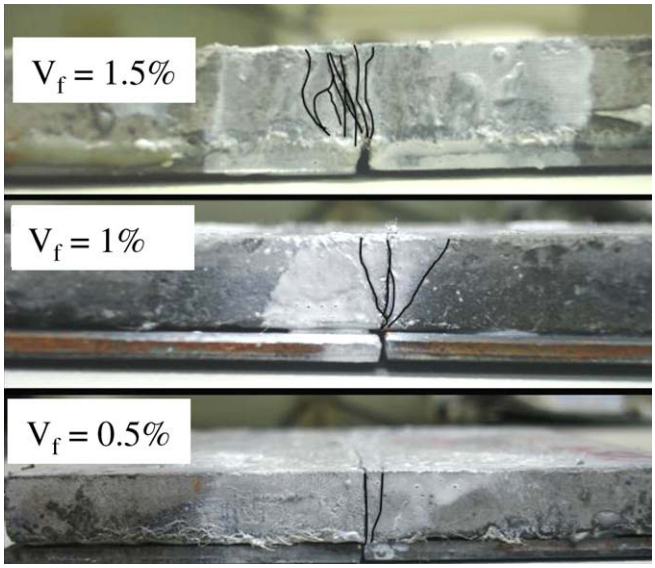

Fig. 9. Crack pattern obtained from zero-span tensile test.

Table 3 shows the averaged crack opening obtained from the zero-span tensile tests and the standard deviation between results. The evaluated crack opening became larger with increasing of the volume fraction of fibers. The material of UHP-SHCC(1.5) has higher ductility than those of UHP-SHCC(1.0) and UHP-SHCC(0.5), as was clarified by uniaxial tensile tests shown in Fig. 3. The crack opening value of UHP-SHCC(1.5) obtained from zero-span tensile test, however, was quite similar to that of UHP-SHCC(1.0). About the crack pattern, Fig. 9 shows the crack pattern observed from the zero-span tensile tests. As shown in this figure, most cracks were adjacent to the artificial crack and the number of cracks depended also on the fiber content in the material.

5. Flexural tests of RC beams repaired by UHP-SHCC

5.1. RC beams as substrates

Six reinforced concrete (RC) beams with length of 1800 mm and cross-section of 100 × 200 mm were prepared. Table 1 shows the mix proportions of the concrete for the substrate. Water to cement ratio was 0.63. Two rebars of D10 (SD295A) were used as the longitudinal reinforcement of each beam. Stirrups of D6 (SD295A)

were used in the shear span at an interval of 90 mm to avoid shear failure of the RC beams, as shown in Fig. 10. For the D10 rebar, the tested yield strength and ultimate strength were 360 and 510 MPa, respectively, and the Young's modulus was 200 GPa.

5.2. Initial loading

After the casting of concrete, the beam specimens were demoulded at 2 days, and the bottom surface of beams was washed out by using a retarder to obtain a roughened surface to ensure perfect bond with the repair material. Then the specimens were covered with wet towels for a curing period of 14 days. By conducting compression tests on three cylindrical specimens of ∅ 100 × 200 mm at 14 days after casting, the averaged compressive strength and Young's modulus were 23.5 MPa and 21.1 GPa, respectively. To induce some cracks in the beam specimens, beams were loaded under four-point bending setup at 14 days after casting, which is named as the initial loading. In all tests, the lengths of the moment and shear spans were 600 and 450 mm, respectively, as shown in Fig. 10. When the average load point displacement exceeded 2 mm, the loading was terminated. Some cracks were detected within the constant-moment span. The detected crack widths due to this initial loading ranged from 0.05 to 0.15 mm.

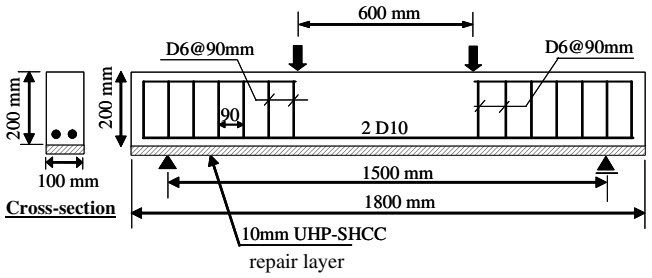

Fig. 10. Reinforcement details of repaired RC beams and test setup.

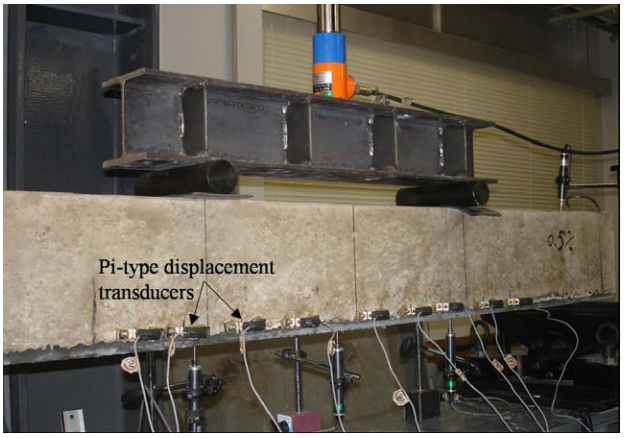

Fig. 11. Second loading setup for repaired RC beams and cracks opening measurements.

5.3. Repair procedure and second loading

After the initial loading, a UHP-SHCC repair layer was placed on the bottom side of the cracked beams. The thickness of the repairing layer was 10 mm, which is the same thickness as that of both the dumbbell-shaped specimens of the uniaxial tensile tests and the zero-span tensile test specimens, as described in the previous sections. The three types of UHP-SHCCs were adopted as repair materials, and two replicate specimens were prepared for each kind. After demoulding of the repaired beam specimens, the specimens were covered with wet towels for 14 days. At 14 days after casting of the repair layer, beams were loaded again in the four-point bending setup. At each crack induced by the initial loading, Pi-type displacement transducer was fixed to measure the crack opening, in addition to the load–displacement curves, as shown in Fig. 10. These transducers had a measurement length of 50 mm and capacity of ±2 mm. At the time of this second loading, the compressive strength and Young's modulus of the substrate concrete were 27.4 MPa and 25 GPa, respectively. Table 2 shows the mechanical properties of the UHP-SHCCs at an age of 14 days, which corresponds to the time of second loading (see Fig. 11).

5.4. Test results

Fig. 12 shows the load–displacement curves of the repaired RC beams. The effect of the different UHP-SHCCs as a repair material on the load–displacement curves was not observed because of

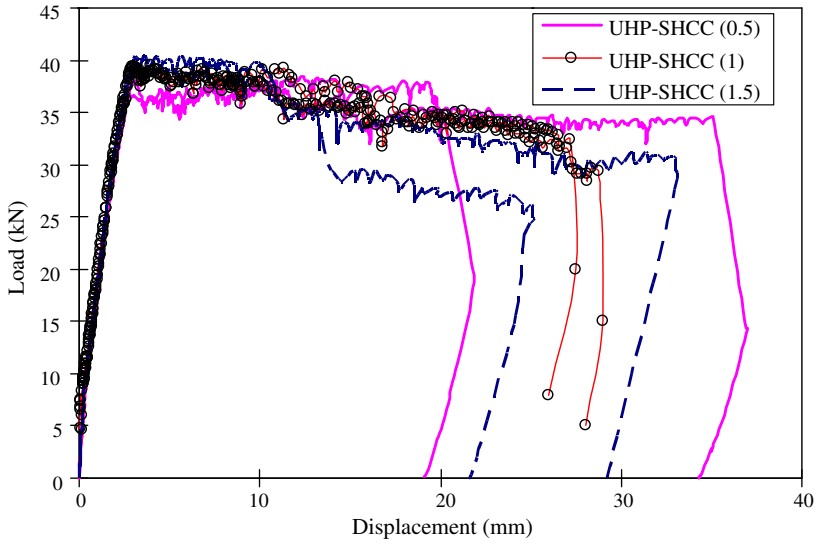

Fig. 12. Load–displacement curves of RC beams repaired by different UHP-SHCCs.

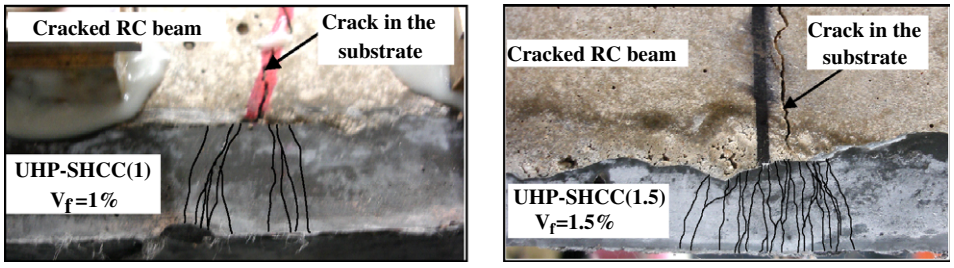

Fig. 13. Crack distributions within repair layers adjacent to existing cracks.

the small thickness of the repair layer relative to the beam depth. Fig. 13 shows examples of crack patterns of the repairing layer observed during the second loading. As shown in Fig. 13, the crack distributions within the repairing layer were adjacent to existing cracks of the repaired RC beams, and the number of cracks increased with increasing fiber content of the repair materials. At the final stage of the loading it was observed that only one crack was completely opened. In Fig. 14, the crack opening value of the localized crack measured by the Pi-type displacement transducers was taken and plotted with the average load point displacement. As shown in Fig. 14, in all specimens the slope of displacement–crack opening curve suddenly increased around a crack opening of about 0.2 mm, and this behavior indicated that localized fracture of the repair material (UHP-SHCC) had occurred. These breaking points can be defined as crack opening of the repair material observed in the repaired RC beams.

6. Comparison of test results and discussion

In this section, the results obtained from the above three tests (i.e. uniaxial tensile tests, zero-span tensile tests, and flexural tests of RC beams repaired by UHP-SHCCs) are compared in terms of their crack patterns and width of cracked region, and crack opening performance.

6.1. Crack patterns and width of cracked region

For the crack patterns of the uniaxial tensile tests, shown in Fig. 4, the cracks were widely distributed along the specimen length. However, the cracked regions in both the zero-span tensile tests and flexural tests of repaired beams were only adjacent to the existing cracks (or artificial crack) in those two test cases. The width of the cracked regions in both tests was quite limited

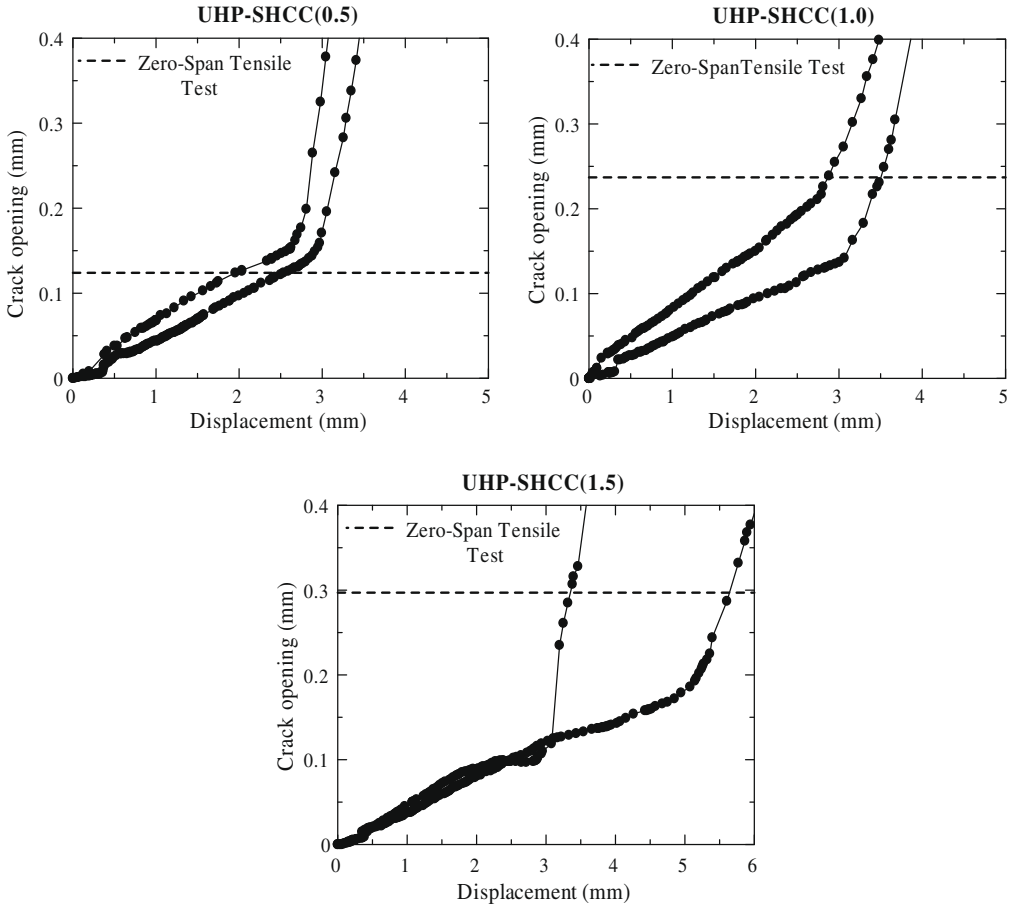

Fig. 14. Crack opening versus displacement at loading points of the repaired beams.

compared to that of the uniaxial tensile tests. The difference in crack pattern became more significant with increasing of fiber content as the UHP-SHCC material could not propagate cracks freely in the flexural tests and zero-span tensile tests, but rather only around the existing crack, as shown in Figs. 9 and 13. It seems that the width of the cracked region depends mainly on the boundary condition of having an existing crack, which of course affects on the crack opening capacity of the tested material, not only on the material properties, as given by uniaxial tensile test. Table 4 shows the averaged width of the cracked region in both the zero-span tensile tests and flexural tests of repaired RC beams, along with the minimum and maximum values of the measurements. Here, the specimens of UHP-SHCC(1.5) and UHP-SHCC(1.0) were only measured, as only one or two cracks were propagated adjacent to the existing crack in case of UHP-SHCC(0.5). The width of cracked parts in both the zero-span tensile tests and flexural tests of repaired specimens were mostly similar to each other, and it can be concluded that the proposed zero-span tensile tests can represent the cracking behavior in repair applications, at least in terms of crack patterns.

6.2. Crack opening performance

For the crack opening performance, the evaluated crack opening performances by the zero-span tensile tests are also plotted in Fig. 14 by dashed lines. As seen in Fig. 14, the crack opening performances obtained from the zero-span tensile tests are mostly similar to those of the repaired RC specimens. By comparing crack opening performance values obtained from uniaxial tensile tests with those obtained from zero-span tensile tests, for the same strain gauge length (50 mm), the crack opening of the uniaxial tensile tests was 2.3 times that obtained from zero-span tensile tests for UHP-SHCC(0.5) case. For UHP-SHCC(1) and UHP-SHCC(1.5) cases, the crack openings of the uniaxial tensile tests were 3.8 and 5 times that obtained from zero-span tensile tests, respectively. In the case of UHP-SHCC(1.5), the effect of the artificial crack on the localized fracture seems to be more significant than for the other cases. This means that the strain capacity and crack opening of a material depends also on the boundary conditions of the loading not only on the material properties according to a uniaxial tensile test.

It was recognized that the strain capacity in uniaxial tensile tests and the crack opening in zero-span tensile tests increase with increasing of fiber volume fraction. However, the point is that the strain capacity in uniaxial tensile tests is more strongly affected by increasing the fiber volume fraction compared to the opening in zero-span tensile tests, as shown in Fig. 15.

According to the zero-span tensile tests results, cracking behavior of the repair material with an existing crack can be roughly estimated. On the other hand, the deformation capacity through the uniaxial tensile tests does not reflect the actual behavior of cracking in the repair material in surface repair application. So the deformation capacity through the uniaxial tensile tests cannot be applied directly to the design of surface repair application.

Regarding the use of the zero-span tensile test method, the degree of opening of the cracks in substrate should be measured or estimated first, and then this value should be compared with the crack opening performance of the repair material obtained from the proposed zero-span tensile test. According to this comparison, the repair material should be selected. Such comparisons provide an effective means for designing and selecting SHCC materials for surface repair applications.

Table 4
Width of cracked region along the tensile direction

Material	Test	Averaged width of cracked part (mm)
UHP-SHCC(1), V_f = 1%	Zero-span tensile test	16.5 (min 11–max 20)
	Flexural test of repaired RC beam	12.8 (min 5–max 20)
UHP-SHCC(1.5), V_f = 1.5%	Zero-span tensile test	20 (min 15–max 30)
	Flexural test of repaired RC beam	20 (min 10–max 40)

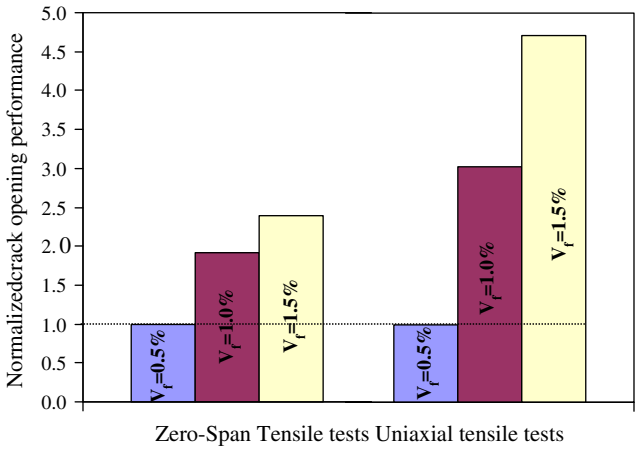

Fig. 15. Effect of fiber volume content on the results of uniaxial tensile tests and zero-span tensile tests (normalizing factor is the crack opening performance of the UHP-SHCC(0.5) case).

7. Conclusions

In this study, the crack opening performance of a repair material with strain hardening behavior was assessed through uniaxial tensile tests, zero-span tensile tests, and flexural tests of RC beams repaired by UHP-SHCC. Following conclusions can be made:

(1) From the viewpoint of cracking behavior
- Cracking behavior of the repair material placed over an existing crack was similar to that of the zero-span tensile tests.
- The width of cracked regions in both the zero-span tensile tests and flexural tests of repaired RC specimens was quite limited compared to that of the uniaxial tensile tests.
- By increasing the fiber volume content in UHP-SHCC, the number of cracks and the deformation capacity increase in both the uniaxial tensile tests and zero-span tensile tests. However, the contribution of increasing the fiber content in the zero-span tensile tests was limited compared to the uniaxial tensile test, as cracking in the zero-span tensile tests is restricted to a small region around the artificial crack.

(2) From the viewpoint of crack opening
- The crack opening obtained from the zero-span tensile tests was similar to that of the flexural tests of repaired RC specimens. For both cases, the deformation capacity was much smaller than that of the uniaxial tensile tests.
- Crack opening and cracking behavior of the SHCC repair material placed over an existing crack can be estimated through the proposed zero-span tensile test.
- The deformation capacity obtained through the uniaxial tensile tests cannot be applied directly to the design of surface repair applications.

References

[1] Lim YM, Li VC. Durable repair of aged infrastructures using trapping mechanism of engineered cementitious composites. J Cem Concr Compos 1997;19(4):373–85.

[2] Shin SK, Kim JJH, Lim YM. Investigation of the strengthening effect of DFRCC applied to plain concrete beams. J Cem Concr Compos 2007;29(6):465–73.

[3] Li VC, Horikoshi T, Ogawa A, Torigoe S, Saito T. Micromechanics-based durability study of polyvinyl alcohol-engineered cementitious composite (PVA-ECC). ACI Mater J 2004;101(1):242–8.

[4] Proceedings of the JCI international workshop on ductile fiber reinforced cementitious composites (DFRCC), Japan Concrete Institute, October 2002.

[5] Kunieda M, Rokugo K. Recent progress of SHCC in Japan – required performance and applications. J Adv Concr Technol, Jpn Concr Inst 2006;4(1):19–33.

[6] Lim YM, Li VC. Durable repair of aged infrastructures using trapping mechanism of engineered cementitious composites. J Cem Concr Compos 1997;19(4):171–85.

[7] Horii H, Matsuoka S, Kabele P, Takeuchi S, Li VC, Kanda T. On the prediction method for the structural performance of repaired/retrofitted structures. In: Proceedings FRAMCOS-3. Fracture mechanics of concrete structures. Freiburg (Germany): AEDIFICATIO Publishers; 1998. p. 1739–50.

[8] Li VC. ECC for repair and retrofit in concrete structures. In: Fracture mechanics of concrete structures. Proceedings FRAMCOS-3. Freiburg (Germany): AEDIFICATIO Publishers; 1998. p. 1715–26.

[9] Li VC, Horii H, Kabele P, Kanda T, Lim YM. Repair and retrofit with engineered cementitious composites. Int J Eng Fract Mech 2000;65(2–3):317–34.

[10] Kamada T, Li VC. The effects of surface preparation on the fracture behavior of ECC/concrete repair system. J Cem Concr Compos 2000;22(6):423–31.

[11] Li VC. High performance fiber reinforced cementitious composites as durable material for concrete structure repair. Int J Restor Build Monuments 2004;10(2):163–80.

[12] Kunieda M, Kamada T, Rokugo K, Bolander JE. Localized fracture of repair material in patch repair systems. In: Proceedings of FRAMCOS-5, Vail, Colorado, USA, April 2004. p. 765–72.

[13] Rokugo K, Kunieda M, Lim SC. Patching repair with ECC on cracked concrete surface. In: Proceedings of ConMat'05, Vancouver, Canada, August 22–24, 2005.

[14] Kamal A, Kunieda M, Ueda N, Nakamura H. Development of a zero-span tensile test for HPFRCC used for structural repairing. In: Proceedings of FRAMCOS-6, CATANIA, Italy, June 17–22, 2007. p. 1509–15.

[15] Kunieda M, Denarié E, Brühwiler E, Nakamura H. Challenges for strain hardening cementitious composites – deformability versus matrix density. In: Proceedings of the fifth international RILEM workshop on HPFRCC, 2007. p. 31–8.

[16] JSCE. Test method for opening performance of concrete surface coating materials over concrete crack (JSCE-K-532-1999). Standard specification for concrete structures. Test methods and specification, March 2002. p. 247–50.